

## **PHASE-CHANGE MATERIAL HEAT EXCHANGER WITH COIL TUBES - EXPERIMENT AND NUMERICAL ANALYSIS**

**Nijaz Delalić, Berina Delalić, Muris Torlak  
Mašinski fakultet Sarajevo  
Vilsonovo šetalište 9, 71000 Sarajevo  
Bosnia-Herzegovina**

### **ABSTRACT**

*Thermal energy storage in a vertically oriented, phase-change material (PCM) filled coil heat exchanger is investigated through experiments and numerical calculations based on computational fluid dynamics (CFD). History of temperature at a number of monitoring points, heat transfer rate and change of solid/liquid phase fractions during the melting and solidification process are recorded. In the melting stage (charging) acceptable agreement of experimental results and numerical prediction is observed. During the solidification process (discharging), shrinkage of PCM triggered by cooling is seen, resulting in air gaps between the heat-transfer pipe and storage medium, which makes heat transfer limited.*

**Keywords:** energy storage, latent heat thermal energy storage (LHTES), phase-change materials (PCM), heat exchanger, computational fluid dynamics (CFD)

### **1. INTRODUCTION**

Storage of thermal energy strongly supports increase of energy efficiency in a number of technical applications, e.g. renewable energy source technologies, particularly solar-thermal power plants, waste-heat management, or indoor climate control. Application of phase-change materials (PCM) as storage medium is attractive, because it enables storage of large amounts of energy within narrow temperature intervals. Previous investigations have shown that numerical prediction based on computational fluid dynamics (CFD) methods can be applied to the analysis of melting of PCM [8]. This paper presents some results of experimental and numerical investigation of thermal energy storage in a coil-tube heat exchanger. Both charging (melting) and discharging (solidification) process are considered.

### **2. EXPERIMENTAL STUDY**

The scheme of the experimental apparatus is shown in Figure 1. Phase-change material heat exchanger with coil tubes experimental apparatus has been developed on the basis of the apparatus for testing of heat exchangers. The experimental setup consists of a system for the preparation of hot water (A), a system for the preparation of cold water (B), the test sections (C) and systems for measurement and data acquisition (D). Figure 2 illustrates the test section, which shows the position of thermocouples for measuring the temperatures. The test section provides measurements for the inlet water temperature and outlet water temperature of the heat exchanger ( $t_{f-in}$ ,  $t_{f-out}$ ). The inner wall temperature distribution of the test section is measured by three chromel-alumel thermocouples ( $t_{w1}$ ,  $t_{w2}$ ,  $t_{w3}$ ). Three thermocouples located in the central axis of the heat exchanger measure temperatures of PCM in the vertical axis ( $t_{b1}$ ,  $t_{b2}$ ,  $t_{b3}$ ). Next to the temperature measurement, mass flow of hot and cold water is measured by two rotameters. These flow meters have a range from 0 to 2 l/h and accuracy of  $\pm 2\%$ .

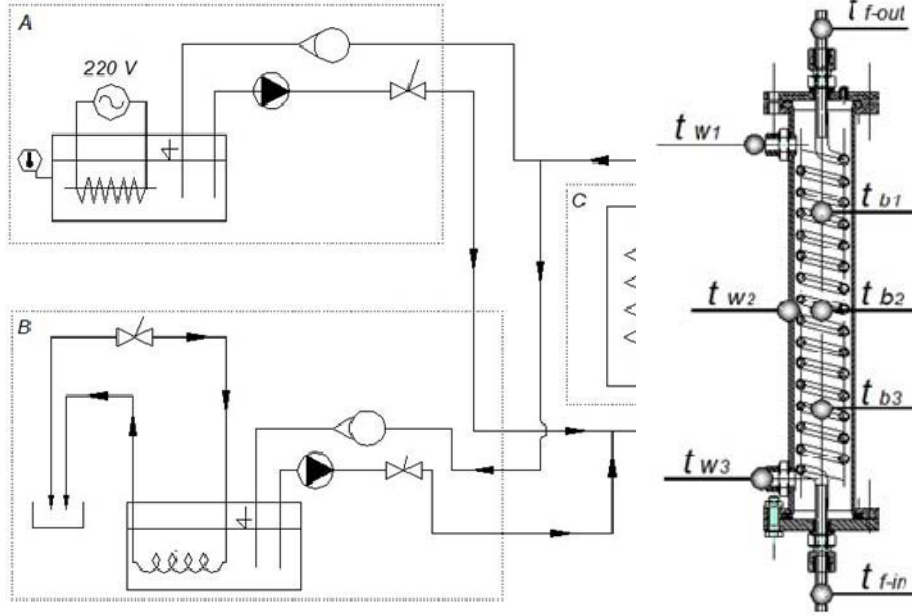


Figure 1. Experimental setup of heat exchanger with coil tubes with Phase-change material: A-preparation of hot water, B-preparation of cold water, C-test section, D-system for measurement and data acquisition

Figure 2. Test section, with position of thermocouples for measuring the temperature

When charging process – PCM melting – is investigated, the hot water flows through the heat exchanger coil, and temperatures at previously mentioned positions are measured. The time period during which the PCM melts is of great importance here. Solidification of PCM is monitored by running the cold water through the heat exchanger coil and measuring relevant parameters with respect to time.

### 3. NUMERICAL METHOD

Heat transfer inside the storage medium as well as flow of the liquid phase are determined by conservation equations of mass, momentum and energy [3]:

$$\frac{d}{dt} \int_V \rho dV + \oint_S \rho \vec{v} d\vec{S} = 0 \quad , \quad \dots (1)$$

$$\frac{d}{dt} \int_V \rho \vec{v} dV + \oint_S \rho \vec{v} \otimes \vec{v} d\vec{S} = -\oint_S p d\vec{S} + \oint_S \vec{\tau} d\vec{S} + \int_V \vec{f}_V dV \quad , \quad \dots (2)$$

$$\frac{d}{dt} \int_V \rho h dV + \oint_S \rho h \vec{v} d\vec{S} = \oint_S \lambda \text{grad} T d\vec{S} + \int_V q dV \quad , \quad \dots (3)$$

where  $\rho$  is the density of the material,  $\vec{v}$  is the velocity vector,  $\vec{S}$  is the control surface,  $V$  is the volume within the control surface,  $t$  is the time,  $p$  is the pressure,  $\vec{\tau}$  is the stress tensor related to the strain rate through an appropriate constitutive relation,  $\vec{f}_V$  is the vector of body forces (for buoyancy effects),  $h$  is the specific enthalpy,  $\lambda$  is the thermal conductivity,  $T$  is the temperature, and  $q$  is the heat source or sink. The specific enthalpy  $h$  arising in eq. (3) is described as:

$$h = \int_{T_0}^T c_p dT + (1 - f_s) H_L \quad , \quad \dots (4)$$

with  $c_p$  being the specific heat capacity,  $H_L$  the latent heat of phase change, and  $f_s$  the volume fraction of the solid phase [7]. Variation of the volume fraction  $f_s$  in the temperature range between solidus and liquidus state is assumed to be linear between 0 and 1. The conservation equations are established for each control volume represented by cells in the numerical mesh, building thus systems of

equations solved sequentially in turn for velocity, pressure (in the liquid phase) and temperature (in both phases) at the cell centers. The equation discretization is based on finite-volume approach which allows the use of cells with arbitrary number of bounding flat faces [2] and [7].

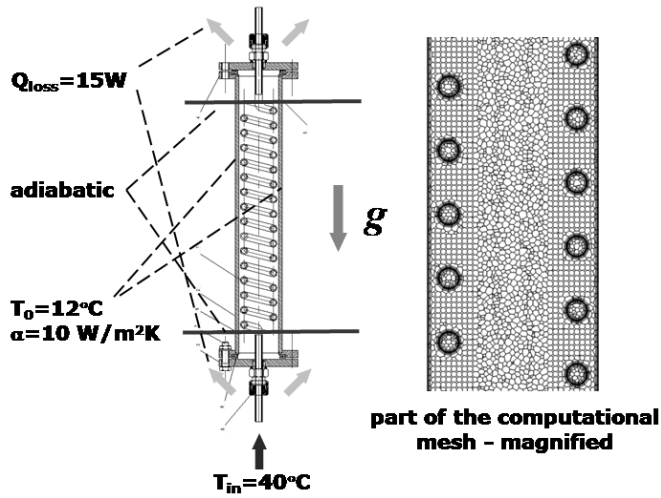


Figure 3. Model of heat exchanger with the boundary conditions from the melting experiment (left). The computational mesh contains

Simulation model with the boundary conditions from the melting experiment and a part of the 3D mesh is illustrated in Figure 3. The heat losses at the entrance and the exit pipe are estimated by comparing the measured total heat loss in the heat transfer fluid (HTF) and estimated heat transfer rate through the outer cylindrical wall of the heat exchanger.

Physical properties of HTF (water) and PCM (Rubitherm RT 27) used in simulation of melting process are given in Table 1. The PCM properties are obtained from [6, 1, 4, 5].

Table 1 Physical properties of HTF water and PCM Rubitherm RT 27 used in melting simulations.

HTF material:	Water at 40°C		PCM material:	Rubitherm RT 27	
Density	992	kg/m <sup>3</sup>	Density, solid <sup>1</sup>	880	kg/m <sup>3</sup>
Dyn. viscosity	0.656	mPa s	Density, liquid <sup>1</sup>	760	kg/m <sup>3</sup>
Specific heat	4179	J/kgK	Dyn. viscosity, liquid <sup>2</sup>	25...33	mPa s
Therm. cond.	0.63	W/mK	Specific heat, solid <sup>1</sup>	1800	J/kgK
			Specific heat, liquid <sup>1</sup>	2400	J/kgK
			Thermal conductivity	0.2	W/mK
			Therm. exp. coefficient	0.001	K <sup>-1</sup>
			Latent heat	140000	J/kg
			Solidus temperature	26	°C
			Liquidus temperature	28	°C

- 1) Linear variation between the solidus and liquidus temperature assumed, otherwise, constant.
- 2) Defined as a function of temperature.

#### 4. RESULTS

Figure 4 shows melting of PCM in the heat exchanger at an instant of time. The white region in the core of the heat exchanger represents the pure solid phase of PCM, which is seen both in experiment (left) and numerical simulation (right). The thick black line in the simulation results distinguishes mushy region from the pure liquid phase, based on temperature level.

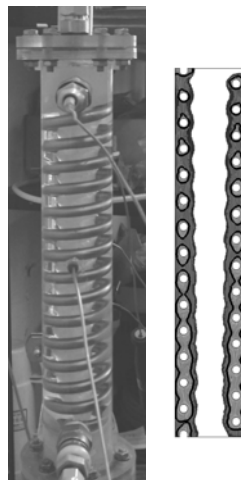


Figure 4. Melting of PCM around the coil tube: photo and picture from simulation

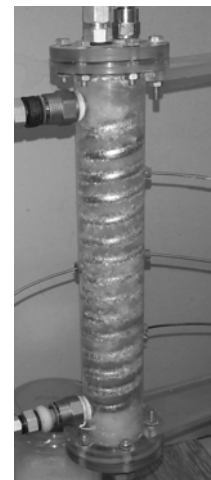


Figure 5. Solidification of PCM in the heat exchanger at an instant of time

Figure 5 shows the process of solidification of PCM, which starts nearby the coil of heat exchanger. Once the PCM mass close around the coil is solidified, a decrease in volume creates an air gap between the narrow layer of solidified PCM and surrounding liquid PCM. Consequently, the process of PCM solidification significantly slows down, due to the reduction of heat transfer from the liquid to solidified PCM, and further to the cold tube of heat exchanger. The left diagram within Figure 6 shows that the PCM temperature on the inside of heat exchanger shell almost equalizes with the temperature of cold water. At the same time it can be seen that the curve of change of temperature in the center of PCM declines very slightly. It is almost uncertain whether this temperature would get closer to the temperature of cold water in coil in a reasonable period of time.

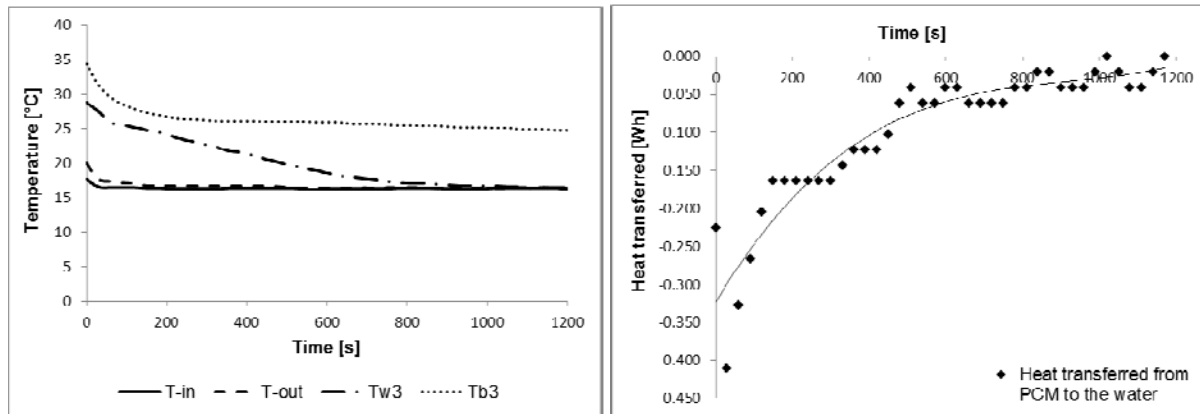


Figure 6. Solidification of PCM: temperature history at inlet, outlet and two monitoring points (left) and history of heat transfer from PCM to the water (right). The heat transfer significantly reduces after about 600 s, which coincides with air gap formation.

## 5. CONCLUSIONS

The process of melting of the PCM is unrestricted in time. The duration of the PCM melting is acceptable. However the PCM solidification is more difficult, due to the air gaps that form during the process and impede the heat transfer from liquid to solid PCM. Possible solution to this problem might be found in increase of number of tubes in heat exchanger which would be surrounded by PCM.

## 6. REFERENCES

- [1] C. Castello, E. Guenther, H. Mehling, S. Hiebler and L. F. Cabeza (2008): "Determination of the enthalpy of PCM as a function of temperature using a heat-flux DSC—A study of different measurement procedures and their accuracy". *Int. J. Energy Res.*, 32, 1258–1265.
- [2] I. Demirdžić, S. Muzafertija (1995): „Numerical method for coupled fluid flow, heat transfer and stress analysis using unstructured moving meshes with cells of arbitrary topology“. *Comp. Meth. Appl. Mech. Engrg.*, 125, 235-255.
- [3] J. Ferziger, M. Perić (2013): *Computational Methods for Fluid Dynamics*, 3rd ed. Springer.
- [4] F. S. Karathia (2011): "Analysis of thermal properties of phase change materials (PCM) using differential scanning calorimeter (DSC)". MSc. thesis, Universitat de Lleida.
- [5] P. Losada-Pérez, C.S. Pati-Tripathi, J. Leys, G. Cordoyiannis, C. Glorieux, J. Thoen (2011): "Measurements of Heat Capacity and Enthalpy of Phase Change Materials by Adiabatic Scanning Calorimetry". *Int. J. Thermophys.* 32, 913–924.
- [6] Rubitherm (2014): Phase Change Material – RT27. <http://www.rubitherm.de/>, last access: 11/30/ 2014.
- [7] A. Teskeredžić, I. Demirdžić, S. Muzafertija (2002): "Numerical method for heat transfer, fluid flow, and stress analysis in phase-change problems". *Numerical Heat Transfer, Part B*, 42, 437-459.
- [8] M. Torlak, A. Teskeredžić, N. Delalić (2013): "Modelling and Simulation of Heat Storage in Phase-Change Materials Based on Computational Fluid Dynamics, 17th International Research/Expert Conference "Trends in the Development of Machinery and Associated Technology", TMT 2013, Istanbul, Turkey, September 2013
- [9] M. Torlak, N. Delalić, B. Duraković, H. Gavranović (2014): "CFD-based assessment of thermal energy storage in phase-change materials (PCM)", *Energy Technologies Conference ENTECH '14*, Istanbul 2014.